Silicon Carbide Fiber-Reinforced Silicon Nitride Composites

Ramakrishna T. Bhatt
U.S. Army Vehicle Technology Center
NASA Glenn Research Center
Cleveland, OH 44135
Phone# (216)433-5513
Ramakrishna.T.Bhatt@grc.nasa.gov

Abstract

The fabrication and thermo-mechanical properties of SiC monofilament- and SiC fiber tow-reinforced reaction-bonded silicon nitride matrix composites (SiC/RBSN) and fully dense SiC monofilament-reinforced silicon nitride matrix composites (SiC/Si_3N_4) have been reviewed. The SiC/RBSN composites display high strength and toughness, and low thermal conductivity in the as-fabricated condition, but are susceptible to internal oxidation and mechanical property degradation in the intermediate temperature range from 400 to 1100^0C. The internal oxidation problem can be avoided by applying functionally graded oxidation resistant coatings on external surfaces of the composite. On the other hand, the fully dense SiC/Si_3N_4 composites fabricated by using SiC monofilaments and pressure assisted sintering methods display moderate strength and limited strain capability beyond matrix cracking stress. Advantages, disadvantages, and potential applications of SiC fiber-reinforced silicon nitride matrix composites fabricated using various fiber types and processing methods are discussed.

I. Introduction

The realization of improved efficiency for engines used for aero and space propulsion as well as for land-based power generation will depend strongly on advancements made in the upper use temperature and life capability of the structural materials used for the engine hot-section components. Components with improved thermal capability and longer life between maintenance cycles will allow improved system performance by reducing cooling requirements and life-cycle costs. This in turn is expected to reduce fuel consumption, to allow improved thrust-to-weight and performance for space and military aircraft; and to reduce emissions and power costs for the electrical power industry.

Currently, the major thrust for achieving these benefits is by the development of fiber-reinforced ceramic matrix composites (FRCMC). These materials are not only lighter and capable of higher use temperatures than state-of-the-art metallic alloys (~1100°C), but also capable of providing significantly better static and dynamic toughness than monolithic ceramics while maintaining their advantages; namely, high temperature strength, low density, erosion and oxidation resistance. However, FRCMC are more difficult to process than monolithic ceramics. The requirement for stable multifunctional fiber-matrix interfaces for optimized composite mechanical properties combined with the relative instability of many fibers with respect to temperature, atmosphere, and chemical interaction with the matrix places stringent limitations on FRCMC processing temperatures and times. For the last twenty years, a variety of FRCMC such as silicon carbide fiber reinforced silicon nitride, silicon carbide fiber reinforced silicon carbide and alumina fiber reinforced alumina matrix composites have been developed. This review covers only SiC fiber-reinforced silicon nitride matrix composites. The other composite systems will be discussed in other chapters of this hand book.

The interest in development of SiC/Si_3N_4 composites stems from the fact that: (a) SiC and Si_3N_4 are thermodynamically compatible and stable at temperatures to 1700^0C, (b) silicon nitride processing temperature can be tailored to avoid fiber degradation, (c) silicon nitride matrix microstructure can be controlled to improve composite properties such as matrix cracking strength and thermal conductivity.

The fabrication of SiC fiber reinforced Si_3N_4-matrix begins by the use of monofilaments, fiber tows, and textile processes (weaving, braiding) to form multi-fiber bundles or tows of ceramic fibers into 2D and 3D fiber architectures or preforms that meet product size and shape requirements. For assuring crack deflection between the fibers and final matrix, a thin fiber coating or interphase material with a mechanically weak microstructure, such as boron nitride (BN) or pyrolytic carbon is then applied to the fiber surfaces by chemically vapor infiltration (CVI). Silicon nitride-based matrices are then formed within the coated preforms by a variety processes: (1) CVI of precursor ammonia and silicon-containing gases that react on the preform surfaces to leave a dense Si_3N_4 product; (2) reaction-bonded silicon nitride (RBSN) where silicon powder in the fiber preform is converted to silicon nitride matrix; (3) polymer infiltration and pyrolysis (PIP) in which a pre-ceramic Si_3N_4-forming polymer is repeatedly infiltrated into open porosity remaining in the composite preform and then pyrolyzed by high-temperature thermal treatments; (4) hot pressing (HP) and (5) hot-isostatic pressing (HIP) in which fiber preform filled with silicon nitride powder and sintering additives is uniaxially or iso-statically pressed at high temperatures.

The pressureless sintering method commonly used for the fabrication of monolithic silicon nitride ceramics cannot be successfully adapted for the fabrication of SiC fiber reinforced silicon nitride matrix composites because of significant strength degradation of currently available fibers at

the high temperatures required for sintering, and also because of the problems associated with retardation of densification of the matrix material by the presence of already dense fibers. Fabrication of SiC/Si_3N_4 composites by CVI was not successful because of the difficulty of maintaining stoichiometry of silicon nitride, and infiltrating into thick sections of the preforms. Also, the textile process for the manufacture of 2-D woven and 3-D braided SiC/Si_3N_4 has not been investigated. Only SiC monofilament- and SiC fiber tow-reinforced Si_3N_4 matrix composites fabricated by reaction-bonding, or hot pressing, or hot-isostatic pressing have been reported in the ceramic literature.

II. SiC Fiber-Reinforced Reaction-Bonded Silicon Nitride Composites

Fabrication of a fiber reinforced reaction-bonded silicon nitride involves heating a fiber-reinforced porous silicon powder preform in pure nitrogen or nitrogen containing gas mixtures at high enough temperature for silicon to react with nitrogen to form silicon nitride. The material produced by the process of converting silicon-to-silicon nitride matrix by gas phase reaction is referred to as reaction-bonded silicon nitride (RBSN). The nitrogen gas diffuses from the outer surfaces of the porous fibrous preform towards its center. A slow, controlled increase in processing temperature can result in reacted material filling the internal pores with no shrinkage of the overall body. In order for the reaction to proceed to completion, a continuous pore structure must be maintained for diffusion of nitrogen. If the number of pores and pore channels is decreasing, then the depth to which the reactions may proceed becomes a limitation. The fiber stability, green density of the fiber preform, particle size and purity of silicon powder, purity of the nitriding gas, and the thickness of the preform are some of the important factors that control the nitriding temperature and time. The greater the density, the less the depth to which the reaction may proceed. The nitrided composites generally contain considerable amount of porosity (20 to 40%). However, the shape,

size and distribution of pores in the nitrided composites can be controlled by controlling fabrication variables.

If SiC fiber tows are used as reinforcements, the reaction-bonded silicon nitride process has the advantage of synthesizing SiC/Si_3N_4 composites in potentially complex and large shapes with near net shape capability, reducing or even eliminating, post-consolidation machining. The SiC/Si_3N_4 composite fabricated by the RBSN process has several advantages: (a) absence of shrinkage during consolidation, (b) RBSN process yields materials with higher purities than typical dense silicon nitride containing sintering aids, (c) improved purity of RBSN matrix can permit achievement of high temperature strength and creep resistance in composites, (d) RBSN processing temperatures are frequently much lower and processing times much shorter than for conventional pressure assisted sintering, (e) service temperature limits can substantially exceed processing temperatures, (f) non-equilibrium phase chemistries or combinations of phases that are inaccessible to conventional processing routes can be achieved.

Because RBSN employs gaseous reactants, the SiC/RBSN material tends to have higher levels of frequently interconnected, residual porosity than the SiC/Si_3N_4 composite fabricated by pressure assisted sintering methods. Interconnected residual porosity remains an important issue for two reasons: oxidation and thermal conductivity. Internal oxidation can lead to internal stresses which may cause premature matrix cracking and fiber delamination. Thus, to avoid internal oxidation protective coatings may be necessary for these materials. Thermal conductivity is also a function of matrix porosity. As the porosity increases, thermal conductivity decreases. Therefore, internal porosity may significantly reduce the thermal conductivity of SiC/RBSN composites. The reduced modulus that intrinsically accompanies uniformly distributed porosity

in RBSN matrix facilitates load transfer to reinforcements, and also lowers thermal stresses in properly designed composites.

The reaction-bonding reaction of converting silicon to Si_3N_4 is exothermic and can be difficult to control. Heat management is a significant issue in those reactions that are exothermic because overheating causes loss of microstructural control and phase chemistry of the Si_3N_4 matrix. Even though reactions are normally carried out at relatively low temperatures (~1350^{0}C), the combination of long reaction times and the reactivity of constituents can pose serious detrimental interactions.

The earliest study on SiC fiber-reinforced RBSN was performed by Lindley and Godfrey [1]. Although fabricated composites showed no strength enhancement over unreinforced RBSN, they reported improved work of fracture for the composites by controlling the fiber/matrix interface. The poor strength properties of the composites were attributed to degradation of the SiC fiber at the fabrication temperature. Interest in SiC/RBSN was rejuvenated in the early 1980's because of the need to develop strong and tough ceramic materials. A feasibility study [2-5] investigating the fabrication of SiC fiber-reinforced RBSN composites using small diameter (<20 μm) SiC fiber tows and large diameter (142 μm) SiC monofilament fibers showed mixed results. The SiC monofilament composites showed some improvement in flexural strength, but the SiC fiber tow-reinforced composites did not. Again instability of the SiC fiber tows at the fabrication temperatures and inadequate bonding between the SiC fibers and RBSN matrix are the primary causes for inferior properties. All the above studies used traditional processing methodology and a nitridation cycle developed for monolithic RBSN for the fabrication of RBSN composites. To overcome the fiber degradation problem, a low temperature, short time nitridation cycle was developed by controlling the particle size, hence surface area, of the silicon

powder [6]. Using this nitridation cycle, strong and tough RBSN composites reinforced by monofilament SiC fibers or SiC fiber tows have been fabricated [6-11]. The following sections review the fabrication, properties, and limitations of these materials.

(1) SiC Monofilament-Reinforced RBSN Composite

(1.1) Processing

The SiC fiber monofilaments consist of a SiC sheath with an outer diameter of 142 μm surrounding a pyrolitic graphite-coated carbon core with a diameter of 37 μm. On the surface of the SiC fiber contained two layers of carbon-rich surface coating. Each layer is a mixture of amorphous carbon and SiC.

The steps involved in the fabrication of SiC/RBSN composites are shown in Fig. 1. The details of the composite fabrication procedure were described in Reference 6. The starting materials for composite fabrication were SiC fiber mats and silicon powder cloth. The SiC fiber mats were prepared by winding the SiC fibers with desired spacing on a cylindrical drum. The fiber spacing used depended on the desired fiber volume fraction in the composite. The fiber mats were coated with a fugitive polymer binder such as polymethylmethacralate (PMMA) to maintain the fiber spacing.

For silicon cloth preparation, the attrition-milled silicon powder was mixed with a polymer fugitive binder (Teflon) and an organic solvent (a kerosene based solvent-Stoddard), and then rolled to the desired thickness to produce silicon cloth.

For composite preform fabrication, the fiber mat and the silicon cloth were alternately stacked in a metal die and hot pressed in vacuum furnace at 1000^0C and 69 MPa pressure to remove the fugitive polymer binder. The resultant composite preform was nitrided at 1250^0C for 10 to 24h to convert silicon to silicon nitride matrix. The fabrication time varies with the panel size. The RBSN

matrix shows ~ 60% α-Si_3N_4, 32% β-Si_3N_4, and ~8% excess silicon. The nitrided composite typically contains ~ 25 vol% SiC fibers, 35 to 45 vol% silicon nitride matrix, and 30 to 40 vol% porosity. The average pore volume, relative amounts of open to closed porosity, and the density of the nitrided composites can be manipulated by silicon powder characteristics and consolidation parameters. Generally the higher the preform density the higher will be the nitrided density. The composite fabricated by the above approach shows a uniform distribution of SiC fibers in the RBSN matrix and stable interface coating on the SiC fibers, both of which are essential for attaining high strength and toughness in composites

(1.2) Properties of Monofilament SiC/RBSN composites

(1.2a) Physical and Mechanical Properties

The properties of a SiC/RBSN composite depend on the volume fraction of the constituents and the bonding between SiC fibers and the RBSN matrix. The room temperature tensile stress-strain curves for the SiC/RBSN composites and the unreinforced RBSN matrix are shown in Fig. 2. The stress-strain curve for the unreinforced RBSN matrix shows only an initial linear elastic region and no strain capability beyond matrix fracture. In contrast, the room temperature tensile stress-strain curves for the 1-D and 2-D SiC/RBSN composites display three distinct regions: an initial linear elastic region, followed by a non-linear region, and then a second linear region. The non-linearity in the stress- strain curve is due to matrix micro-cracking normal to the loading direction. The strain capability beyond initial matrix fracture is possible because of the weak or frictional bond formed between the fiber and RBSN matrix and the retention of a large fraction of as-produced fiber strength under the fabrication conditions. If the fibers were strongly bonded to the matrix, the composite would have behaved similar to that of the unreinforced matrix.

The slope of the initial elastic portion of the stress-strain curve represents Young's modulus, which primarily depends on volume fraction and elastic modulus of the fibers and the matrix. Theoretically, Young's modulus (E_C) of the composite can be estimated using the rule-of-mixtures.

$$E_C = E_f V_f + E_m V_m$$

Where E is the elastic modulus, V is volume fraction of the constituent, and the subscripts f and m refer to the fiber and matrix, respectively. The elastic modulus of the RBSN matrix decreases with increasing porosity. To estimate the elastic modulus of RBSN with known porosity, the following equation may be used [12].

$$E_m = E_o \exp(-3V_P)$$

Where V_P is the total volume fraction of porosity and E_o is the Young's modulus of dense silicon nitride which has a value of 300 GPa [13].

The slope of the second linear line represents the secondary modulus which is primarily controlled by the fibers. If fibers are not broken until the ultimate tensile strength is reached, the secondary modulus should correspond to $\sim E_f V_f$. A secondary modulus value less than $\sim E_f V_f$ indicates the fracture of fibers in the early stages of deformation.

At the inflection point, a single through-the thickness matrix crack forms normal to the loading direction and the crack occurs at the largest matrix flaw. As the loading is increased beyond the inflection point, the pieces of matrix on both side of the crack load and crack again at the next largest matrix flaw. This process continues until matrix blocks cannot sustain load. The stress at which the first matrix crack forms can be modeled by knowing the volume fractions and elastic moduli of the constituents, interfacial shear strength between the fiber and the matrix, fracture toughness of the matrix, fiber diameter, and nature of residual stress in the composite. Various fracture mechanics-based models can fairly accurately predict the matrix cracking strength.

The ultimate tensile strength of the composite is controlled by the fibers. Therefore, knowing the bundle strength of the fiber, the ultimate tensile strength of the composite, σ_c, can be estimated from the equation,

$$\sigma_C = \sigma_{fB} V_f$$

where σ_{fB} is the fiber bundle strength and V_f is the fiber volume fraction.

The tensile properties of unidirectional SiC/RBSN composites are anisotropic, i.e., in the fiber direction the composite is strong, but in the direction transverse to the fibers it is weaker than even the unreinforced matrix. To achieve isotropic properties, multi directional reinforcement is needed, but the penalty of multi directional reinforcement is reduced mechanical properties as illustrated by the tensile stress- strain curve for the 2-D SiC/RBSN composite (Figure 2). Table I summarizes the room temperature mechanical properties of 1-D and 2-D SiC/RBSN composites.

The SiC/RBSN composites showed several advantages over monolithic Si_3N_4. The room temperature tensile strength properties of unidirectionally reinforced SiC/RBSN composites are relatively independent of tested volume (Fig. 3); whereas the ultimate strength of monolithic ceramics decreases with increasing volume because of greater probability of finding a strength-limiting flaw with increasing volume [8,15]. In other words, the strength of a fiber-reinforced ceramic matrix composite does not depend on the largest flaw formed during fabrication or during specimen preparation, but it depends on the complex interaction of local stress fields around the flaws and their growth due to global stresses. This implies that for applications requiring large material volumes, such as, turbine blades or rotors, the strength of SiC/RBSN composites may be better than that of dense, commercially available hot-pressed Si_3N_4. In addition, SiC/RBSN composites display notch insensitive strength behavior and better impact resistance than unreinforced RBSN or dense Si_3N_4 material.

The variation of tensile strength with temperature in air for a 1-D SiC/RBSN composite is shown in Fig. 4 [16]. The elastic modulus and matrix cracking strength decreases slowly with increase in temperature, but the ultimate tensile strength remains relatively constant from 25 to 600^0C. Beyond this temperature it decreases due to oxidation of the carbon coating on the SiC fibers and creep effects.

(1.2b) Thermal Properties

(1.2b.1) Thermal Expansion

Thermal expansion of unidirectional SiC/RBSN composite is mainly a function of constituents' volume fractions and measurement direction relative to the fiber, and is not affected by constituents' porosity. Measurement of linear thermal expansion with temperature in nitrogen for the 1-D SiC/RBSN composites parallel and perpendicular to the fibers indicates a small amount of anisotropy (Fig. 5). This is attributed to small difference in thermal expansion coefficients of SiC fibers ($4.2x10^{-6}$) and RBSN matrix ($3.8x10^{-6}$) as well as anisotropic thermal expansion of carbon coating on SiC fibers. In the fiber direction, linear thermal expansion is controlled by the SiC fiber, and in the direction perpendicular to the fiber, it is controlled by the RBSN matrix.

Thermally cycling the 1-D SiC/RBSN composites between 25 and 1400^0C in nitrogen had no significant effect on the linear thermal expansion curve transverse to the fibers, but thermal cycling in oxygen caused a positive shift in $((L-L_0)/L_0)$ in the first cycle indicating length (L) increase (Fig. 6). With each additional cycle, a further increase in specimen length was observed, but with each additional cycle, a further increase in specimen length was observed, but the rate of increase in length/cycle consistently decreased. After the third cycle, reproducible thermal expansion curves with no apparent hysteresis were obtained.

Since RBSN is a porous material and most of the porosity is interconnected, exposing it to oxygen results in growth of silica on the geometrical surfaces and the surfaces of pores as well. However, the pore wall oxidation ends quickly with the sealing of the pore channels near the surface because of the 82% increase in volume during conversion of a mole of silicon nitride to a mole of silica. Beyond this stage, oxidation is limited to the geometrical surfaces. During cycling the surface silica layer appears to have cracked due to crystallization and phase transformation. Growth of silica on the pore walls as well as on the external surfaces accounts for length increase in the SiC/RBSN composites.

Internal oxidation of SiC/RBSN is severe between 800 to 1100°C, and the depth of the oxidation damage zone is directly related to the pore size; the smaller the pore size, the lower is the oxidation induced damage. In addition, internal oxidation is also found to generate tensile residual stresses which affect strength properties of SiC/RBSN.

Thermal cycling of SiC/RBSN in nitrogen had no effect on mechanical properties, but in oxygen environment, composite properties degraded due to internal oxidation (discussed in Section 1.2d) and swelling of the composites as shown in Table II.

(1.2b.2) Thermal Conductivity

The influence of temperature on calculated thermal conductivity for 1-D SiC/RBSN composites parallel and perpendicular to the fiber is plotted in Fig. 7. The thermal conductivity (K) was calculated from the equation,

$$K=\rho C_P \alpha$$

where C_P is the specific heat, α is the thermal diffusivity, and ρ is the density of the material. The specific heat, thermal diffusivity, and the density of the material were measured quantities. Thermal conductivity parallel to the fibers is greater than perpendicular to the fibers. Thermal conductivity

generally decreases with temperature. In the fiber direction, both the SiC fiber and the RBSN matrix contribute to the thermal conductivity, whereas in the direction perpendicular to the fiber, thermal conductivity is predominantly controlled by the matrix. The significant difference in thermal conductivity parallel and perpendicular to the fiber is attributed to a boundary gap between the SiC fiber and the RBSN matrix. Existence of a boundary gap has been confirmed by experimental methods [18, 19].

The coefficient of linear thermal expansion, specific heat, thermal diffusivity, thermal conductivity for 1-D and 2-D SiC/RBSN at four temperatures in nitrogen measured parallel and perpendicular to the fibers are summarized in Tables III and IV. In general, through-the thickness thermal conductivity ~~value~~ at room temperature for SiC/RBSN composites is low when compared with a value ~ 7 W/m-k for the unreinforced RBSN or with a value of ~ 30 W/m-k for the sintered silicon nitrides [13]. Both weak bonding between the SiC fiber and the RBSN matrix, and porosity in the RBSN matrix appear to affect the thermal conductivity in this system.

(1.2c) Thermal Shock Resistance

The ability to withstand the thermal stresses generated during ignition, flameout, and operating temperature excursions is an important consideration in evaluating potential high temperature materials. Thermally created stresses may initiate delamination and microcracking or cause existing matrix flaws to grow giving a gradual loss of strength and modulus and eventual loss of component integrity. However, the evaluation of thermal stress resistance is a complex task since performance depends not only on material thermal and mechanical properties, but it is also influenced by heat transfer and geometric factors such as heat transfer coefficient and component size. No reliable testing methods exist to evaluate thermal shock resistance of materials except testing sub-elements in an engine environment. However, the water quench and thermal gradient

tests are used to qualitatively evaluate thermal shock performance of potential high temperature materials.

The thermal shock resistance of unidirectionally reinforced SiC/RBSN composites was evaluated using the water quench method. Both room temperature flexural (Fig. 8) and tensile properties (Fig. 9) of 1-D SiC/RBSN composites were measured before and after quenching and compared with the flexural properties of quenched unreinforced RBSN under similar conditions.

When tested under tensile testing mode, the thermally shocked SiC/RBSN composite showed no loss in tensile properties, but under flexural testing mode, the composites showed loss of ultimate flexural strength after quenches from above 600^0C. The flexural strength loss behavior for the quenched unreinforced RBSN appeared similar to that for the composite, but for unreinforced RBSN, the strength loss occurred after quenches from temperatures above 425^0C which is 175^0C less than that observed for the composite. Although thermal shocking did damage to the composite, probably by microcracking of the matrix, it did not affect the tensile properties of the composite. These results indicate that SiC/RBSN composites have better thermal shock resistance than the unreinforced RBSN and thus better toughness or flaw tolerance.

(1.2d) Environmental Stability

The SiC/RBSN composites are stable in inert environments such as argon, and nitrogen at temperatures to 1400^0C for 100h, but in oxygen, oxidation starts as low as 400^0C [21]. Oxidation effects on unidirectionally reinforced SiC/RBSN composites are shown in Figure 10. Three oxidation regimes have been identified: oxidation of the fiber/matrix interface, oxidation of the porous Si_3N_4, and intrinsic strength degradation of the SiC fibers. At low temperatures between 400-800^0C, where oxidation of porous Si_3N_4 is not kinetically favorable, oxygen could diffuse through the porous matrix and oxidize the carbon coating at the fiber/matrix interface. This reaction

decouples the fiber from the matrix, causing loss of load transfer and loss of strength. In the temperature range between 800^0-1100^0C, where internal oxidation of the porous Si_3N_4 is prevalent, both reactions - formation of silica in the Si_3N_4 pores and oxidation of the fiber/matrix interface - occur simultaneously. Beyond 1100^0C, rapid oxidation of the porous Si_3N_4 matrix allows formation of dense silica on the composite surface which reduces permeability of oxygen through the matrix. However, instability of the fiber surface coating and possible fiber degradation still results in some loss in composite strength.

(1.2e) Creep Properties

Creep resistance is of primary concern in rotating components of a turbine engine. High creep rates can lead to both excessive deformation and uncontrolled stresses. Creep resistance of fiber-reinforced ceramic matrix composites depend on relative creep rates of, stress-relaxation in, and load transfer between constituents. The tensile creep behavior of SiC/RBSN composites containing ~24 vol% SiC monofilaments was studied in nitrogen at 1300^0C at stress levels ranging from 90 to 150 MPa. Under the creep stress conditions the steady state creep rate ranged from $1.2x10^{-9}s^{-1}$ to $5.1x10^{-8}s^{-1}$. At stress levels below the matrix cracking stress, the RBSN matrix has a lower creep rate than the SiC monofilaments. Therefore, SiC/RBSN composites generally show low creep rate at 1300^0C at stress levels up to 120 MPa in inert environments as shown in Fig. 11 [22]. However, because of the high creep resistance of the RBSN matrix, load is shed from SiC monofilaments to the RBSN matrix during creep, leading to progressive increase in matrix stress and a relaxation in fiber stress. This will eventually lead to matrix fracture, and the development of periodic matrix cracks, with load transferred across the cracks by the bridging fibers. This is undesirable from long term creep point of view, since the creep strength of the composite after matrix cracking is now controlled by the rupture strength of the

fibers, which must now support the entire creep load across the crack faces. Exposure of the interface and the fibers to oxygen, in a cracked composite will lead to its premature failure.

(2) Reaction-Bonded Silicon Nitride Systems with Tow Fibers

The SiC/RBSN composites containing SiC monofilaments as discussed earlier cannot be pursued for component manufacturing for three reasons: first, the fact that large diameter fibers cannot be bent to a radius less than 1 mm severely restricted the shape capability for the components; second, machining the components from a block of composite is very expensive and time consuming; third, the SiC/RBSN composites with large diameter fibers did not bridge the matrix cracks effectively. The limitations of large diameter reinforcement can be avoided by employing textile processes (weaving, braiding) to form multi-fiber bundles or tows of ceramic fibers into 2D and 3D fiber architectures. However, fabrication of the 2D and 3D SiC/RBSN has not been fully investigated. Brandt et al [4] fabricated the 2-D SiC/RBSN matrix composites by infiltrating silicon slurry into a stack of 2-D SiC woven cloth, consolidating the stack by hot-pressing, and then reaction-bonding the hot-pressed stack. The strength and density values of the composite were low, and the composite showed moderate improvement in toughness. Few studies reported fabrication of SiC/RBSN composites using SiC fiber tows and prepreg/hotpressing methods of consolidation [2, 3, and 11]. The fabrication and properties of these composites are discussed below.

(2.1) Processing

The as-received fiber tows were spread and coated with a layer of BN and then with a layer of SiC; both layers were deposited by chemical vapor deposition. For the fabrication of SiC fiber tow mats filled with silicon power slurry, the BN/SiC coated SiC fiber tow was passed through a series of rollers to spread the tow and then into a tank filled with the silicon slurry. The slurry

coated fiber tows were wound on a metal drum at a predetermined spacing to prepare fiber mat. Strips, either all-unidirectional or alternate strips of unidirectional and transverse lay-up, were stacked in a die and pre-pressed at 3.5 MPa at room temperature. The pre-pressed composites were hot pressed at 40 MPa at 800°C for 15 min and then the load was released. Subsequently the temperature was increased to 1200°C and the panel was nitrided for 4 h in flowing nitrogen.

(2.2) Properties of Tow SiC/RBSN Composites

Room temperature physical property data for as-processed 1-D and 2-D SiC/RBSN tow composites are shown in Table V. The composites contained ~24 vol% SiC fibers and ~36 vol% porosity.

The room temperature tensile stress strain curves for the 1-D and 2-D SiC/RBSN tow composites and that of the unreinforced RBSN are shown in Figure 12. In general, the composite stress-strain curves showed two regions: a linear elastic region followed by a non linear region. At the inflection point where elastic region changes to non linear region a transverse crack formed normal to the loading direction, but this crack propagated partially into the through-the-thickness direction. This damage mechanism is in contrast to that observed for SiC/RBSN composites reinforced by SiC monofilaments in which only through-the-thickness matrix cracks are formed. As the loading is increased, additional transverse cracks are formed along the gage section specimen until final fracture. The fracture surface indicated significant fiber pull out. The room temperature tensile property data for SiC/RBSN tow composites are tabulated in Table VI.

(3) Oxidation Protection Methods for SiC/RBSN Composites

Internal porosity in SiC/RBSN composites can be controlled but cannot be eliminated during processing of the composites. Interconnected internal porosity is a liability for SiC/RBSN

composites because of poor oxidation resistance in the intermediate temperature range from 400 to 1100^0C and poor thermal cyclic resistance. To avoid the internal oxidation problem several methods such as infiltration of RBSN composites with a silicon nitride-yielding polymer, surface coating the RBSN composites with a layer of CVD SiC or Si_3N_4, or multiple layers of CVD SiC and glass formers have been investigated [23-27]. The SiC/RBSN monofilament composites infiltrated with a silicon nitride-yielding polymer showed better oxidation resistance than uncoated SiC/RBSN composites at temperatures greater than 800^0C in the initial stages of oxidation, but after 100hr exposures, oxidation behavior of polymer infiltrated and uninfiltrated SiC/RBSN composites were the same. During long term exposure at high temperatures, amorphous polymer derived silicon nitride recrystallized, causing shrinkage cracks and porosity which opened the sealed surface for further oxidation. On the other hand, the CVD SiC and glass-former coated SiC/RBSN monofilament composites survived (Fig. 13) both static and cyclic burner rig testing at temperatures to 1600^0C for 10 hrs [28]. The carbon core and carbon-rich coating on the monofilament SiC fibers very close to surface coating were still intact. This suggests that externally coated SiC/RBSN composites can be used for high temperature applications provided the coating is not completely cracked in service conditions.

(4) Sub-Element Testing

Oxidative stability of surface coated SiC/RBSN monofilament composites in burner rig testing prompted interest in utilization of this composite for uncooled components for small engine applications. Turbine vanes were machined from blanks of 1-D and 2-D SiC/RBSN composites, and surface coated with a layer of CVD SiC and glass former. Both uncoated and coated vanes were engine tested in at 1315^0C for 10h. The uncoated vanes showed severe damage, but the surface coated vanes survived engine tests with minimal damage [28].

III. Dense SiC/Silicon Nitride composites

SiC fiber reinforced silicon nitride powder preforms without any sintering additives are difficult to densify by pressure assisted sintering methods because the volume diffusivity of silicon nitride is not large enough to offset the densification retardation effects of surface diffusion and volatilization phenomena. To promote densification, it is necessary to mix silicon nitride powder with sintering oxide additives while fabricating SiC/Si_3N_4 composites. During pressure assisted sintering, the oxide additive reacts with silica on the surface of silicon nitride powder to form complex silicates. One disadvantage of silicates is that they are less refractory than silicon nitride. Therefore, the high temperature properties of SiC/Si_3N_4 composites are controlled by properties of the silicates, and not by silicon nitride. Two major issues with pressure assisted sintering methods are possible degradation of fibers during processing and limited shape capability.

Rice and coworkers [29] fabricated SiC fiber reinforced Si_3N_4 composites by slip casting and hot pressing methods. The processing scheme included dispersion of an array of SiC fibers in silicon nitride slurry to prepare a green material, and followed by hot pressing the green material at ~ 1500^0C for de-bindering and consolidation. The fabricated composites displayed high fracture toughness, but their strengths were moderate in relation to typical strengths achieved in hot-pressed Si_3N_4. Several factors such as non-uniform distribution of the fibers, degradation of the fibers at the high processing temperatures, and incomplete densifications were suggested as reasons for limited strength. Shetty et al [30] reported fabrication of dense SiC/Si_3N_4 composites containing monofilament SiC fibers. A combination of slurry coating and filament-winding was used for processing green monotapes of unidirectional silicon carbide monofilament in silicon nitride powder blend which contained 8 wt% Y_2O_3 and 4 wt% Al_2O_3.

The monotapes were stacked and hot pressed in a die at 1750^{0}C in N_2 atmosphere at 27 MPa. The 3-point flexural strengths of the resulting composites were significantly lower than that of the unreinforced silicon nitride. Crack-initiation resistance of the composites was comparable or only marginally better than that of the Si_3N_4 matrix, but the crack propagation resistance was significantly high. Strength degradation of fibers from exposure to the processing temperature, residual tensile stress, and filament damage during hot pressing are possible factors responsible for poor strength of the composites. Foulds et al [31], improvising the above processing approaches, were able to fabricate fully dense, strong and tough SiC/Si_3N_4. Razzell and Lewis [32] fabricated fully dense SiC/Si_3N_4 composites by post hot-pressing SiC/RBSN composites containing SiC monofilaments and oxide sintering additives. The three-point flexural strength of the composite material was similar to that of the unreinforced silicon nitride, but the composites displayed several toughening mechanisms. Nakano et al [33] reported manufacturing of SiC/Si_3N_4 composites using SiC fiber tows and hot-pressing. Flexural strength and fracture toughness of the composites at room temperature were 702 MPa and 20.2 MPa(m)$^{1/2}$, respectively. The composite degraded when tested at 1400^{0}C. The processing and properties of SiC/Si_3N_4 composites with SiC monofilaments are discussed in the next section.

(1) Processing

SiC monofilaments were collimated and wound on the outside of a revolving drum, where a resin was used to maintain fiber spacing. The fiber/resin mats were sectioned from the drum surface and used as layers between matrix powders in hot pressing. In an alternate processing method, SiC monofilaments were wound on the wax sheet wrapped drum at the desired spacing, and then, a silicon nitride powder blend-filled polymer slurry was sprayed on the monofilament to produce a flexible fiber/matrix tape. This tape can be cut, laid up, and hot

pressed similar to the processing method described above. The drum wrap-spray coat procedure allows for precise fiber spacing and orientation, complete coating of fibers, precise thickness control and scalability to larger structures. The fiber/resin mats were applied sequentially between layers of matrix in a graphite mold. The matrix powder contained 5 wt%Y_2O_3 and 1.25 wt% MgO as densification aids. The preform powder lay up was consolidated at 1700^{0}C under 70 MPa pressure for 1 hr in a vacuum atmosphere. The fabricated composites typically showed a density value of ~3.2 gm/cc, which is the theoretical density for SiC/Si_3N_4 composites containing 30 vol% SiC fibers. Uniform distribution of SiC fiber within the Si_3N_4 matrix was achieved and the carbon coating on the fiber remained intact.

(2) Physical and Mechanical Properties

The room temperature tensile stress strain behaviors of 1-D and 2-D SiC/ Si_3N_4 monofilament composites showed high matrix cracking stress, but strain capability beyond matrix fracture is limited . Limited fiber pull out was observed on the tensile fracture surfaces [31].

Limited property data for HP SCS-6/ Si_3N_4 composites are reported in the literature. The 1-D HP SiC/ Si_3N_4 composite shows ~ 380 MPa and ~ 450-475 MPa matrix cracking strength and ultimate tensile strength, respectively. A 2-D composite is essentially brittle and shows ~300 MPa matrix cracking/ultimate tensile strength. Compilation of physical and mechanical property data from three studies are summarized in Table VII.

(3) Creep Properties

The tensile creep behavior of a HP SCS-6/ Si_3N_4 composite was investigated in air at 1350^{0}C [34, 35]. The unidirectional composite containing 30 vol% SiC monofilaments was creep tested at stress levels at 70,110,150, and 190 MPa (Fig. 15). The steady state creep rate ranged

from an average of $2.5x10^{-10}$ s^{-1} at 70 MPa to $5.6x10^{-8}s^{-1}$ at 150 MPa. The slope of the steady state creep rate vs creep stress curve yields a value of ~7 which is comparable to the stress exponent of 4 to 6 found for tensile creep of monolithic Si_3N_4. For a similar stress, the average steady state creep rate of the composite was ~ four orders of magnitude lower than the tensile creep rate of the HP Si_3N_4. At low stresses, ~70 MPa, creep failure was accompanied by extensive fiber pullout and debonding along the fiber/matrix interfaces. The extent of fiber pullout diminished as the creep stress was increased. For specimens crept at stress levels between 70 and 110 MPa, small fraction of fibers fractured during creep deformation as evidenced by the a small discontinuous strain jumps in the steady state creep regime.

(4) Impact Resistance

Turbine components, specifically vanes and blades, and tank armor, are subjected to impact damage. Therefore, the mechanism of impact damage and consequence of impact damage on strength properties are also important in design of turbine components. To evaluate ballistic impact resistance of HP-SiC/Si_3N_4, Foulds et al [31] impact tested both HP monolithic and 2-D SiC/Si_3N_4 composite tiles. The composite specimens showed local damage, but the monolithic material fragmented completely

IV. Applications

Because of their high specific modulus and strength, toughness, and low thermal conductivity SiC/RBSN composites containing SiC fiber tow reinforcements are potential candidates for uncooled heat engine components such as inter turbine ducts, combustor liners, nozzle vanes, divergent and convergent flaps, and blades. However, these components must be coated with surface coatings to avoid internal oxidation. Other applications include radome, and exhaust nozzles. On the other hand, uses of SiC/RBSN or fully dense SiC/Si_3N_4 composites

containing SiC monofilaments are limited to simple shaped components such as flame holders, divergent and convergent flaps, and high temperature seals.

V. Summary and Concluding Remarks

Various studies indicate that strong, tough, creep and impact resistant SiC/RBSN and SiC/Si_3N_4 composites can be fabricated. The highlights of these studies are the following:

(1) SiC/RBSN composites containing monofilaments are limited to simple shape[5]. However, SiC/RBSN shape capability can be improved by using textile processes (weaving, braiding) to form multi-fiber bundles or tows of ceramic fibers into 2-D and 3-D fiber architectures.

(2) Internal pores in SiC/RBSN composites are unavoidable and reduce their oxidation resistance and thermal conductivity. Functionally graded oxidation resistant surface coatings appear to avoid internal oxidation problems for unstressed conditions.

(3) Fully dense SiC/Si_3N_4 can be fabricated by pressure assisted sintering methods, but the processing methods do not allow complex shape capability. The high temperature fabrication conditions also degrade fiber strength and hence ultimate tensile strength and strain capability. As a result, application potential for dense SiC/Si_3N_4 composites is very limited.

VI. References

[1] M.W. Lindley and D.J. Godfrey, "Silicon Nitride Composites with High Toughness," Nature, 229, 192-193 (1971).

[2] J.W. Lucek, G.A. Rossetti, Jr., and S. D. Hartline, "Stability of Continuous Si-C (-O) Reinforcing Elements in Reaction-Bonded Silicon Nitride Process Environments,"

pp. 27-38 in Metal Matrix, Carbon, and Ceramic Matrix Composites 1985, NASA CP-2406, Edited by J. D. Buckley, NASA, Washington, D.C., 1985.

[3] N.D. Corbin, G.A. Rossetti, Jr., and S.D. Hartline, "Microstructure/Property Relationships for SiC Filament-Reinforced RBSN," Ceram. Eng. Sci. Proc., 10, [9-10], pp. 1083-1089 (1989).

[4] J. Brandt, K. Rundgren, R. Pompe, H. Swan, C. O'Meara, R. Lundberg, and Pejryd, "SiC Continuous Fiber-Reinforced Si_3N_4 by Infiltration and Reaction Bonding," Ceram. Eng. Sci. Proc. 13, [9-10], pp. 622-631 (1992).

[5] T.L Starr, D.L. Mohr, W.J. Lackey, and J. A. Hanigofsky, "Continuous Fiber-Reinforced Reaction Sintered Silicon Nitride Composites," Ceram. Eng. Sci. Proc. 14, [9-10], pp. 1125-1132 (1993).

[6] R.T. Bhatt, "Method of Preparing Fiber Reinforced Ceramic Materials," U.S. Pat. No. 4689188, 1987.

[7] R.T. Bhatt, "Mechanical Properties of SiC/RBSN Composites", in "Tailoring Multiphase and Composite Ceramics," (1986), p. 675 edited by R.E. Tressler, G.L. Messing, C.G. Pantano and R.E. Newnham, Plenum Press, New York.

[8] R.T. Bhatt, "The Properties of Silicon Carbide Fiber Reinforced Silicon Nitride Composites," in Whisker- and Fiber-Toughened Ceramics, (1988) pp. 199-208 edited by R.A. Bradley, D.E. Clark, D.C. Larsen, and J.O. Stiegler, ASM International, Ohio.

[9] R.T. Bhatt and R.E. Phillips, "Laminate Behavior for SiC Fiber-Reinforced Reaction-Bonded Silicon Nitride Matrix Composites," J. Comp. Techn. Res. **12**, p.13, 1990.

[10] R.T. Bhatt and J.D. Kiser, "Matrix Density Effects on Mechanical Properties of SiC/RBSN Composites," NASA-TM 103733, 1990.

[11] R.T. Bhatt, "Tensile Properties and Microstructural Characterization of Hi-Nicalon SiC/RBSN Composites," Ceramics International, #26, pp535-539, 2000.

[12] A.J. Moulson, "Review: Reaction Bonded Silicon Nitride; Its Formation and Properties," J. Mater. Sci., 14, pp 1017-1051, 1979.

[13] S. Hamshire, "Engineering Properties of Nitrides," Engineered Materials Handbook, V1, 1987 ASM International, Metals Park, Ohio 44073.

[14] R.T. Bhatt, "Tension, Compression, and Bend Properties for SiC/RBSN Composites," Proc. of the 8th ICCM Conference Vol. III, 23-A, 1991.

[15] G.K. Bansal and W.H. Duckworth, "Effects of Specimen Size on Ceramic Strength," in "Fracture Mechanics of Ceramics" (1978), 3, p. 189 edited by R.C. Bradt, D.P.H. Hasselman and F.F. Lange, Plenum Press, New York.

[16] J.Z. Gykenyesi, "High Temperature Mechanical Characterization of Ceramic Matrix Composites" NASA CR -206611, 1998.

[17] R.T. Bhatt and A.R. Palczer, "Effects of Thermal Cycling on Thermal Expansion and Mechanical Properties of SiC Fiber-Reinforced Silicon Nitride Matrix Composites," J. Mat. Sci. **32**, 1039-1047, 1997.

[18] H. Bhatt, K.Y. Donaldson, D.P.H. Hasselman, and R.T. Bhatt, "Effect of Finite Interfacial Conductance on the Thermal Diffusivity/Conductivity of SiC Fiber Reinforced RBSN," Thermal Conductivity **21**. 1990, ed. C.J. Cremers and H.A. Fines, Plenum Press, New York, NY.

[19] H. Bhatt, K.Y. Donaldson, D.P.H. Hasselman, and R.T. Bhatt, "Role of Interfacial Thermal Barrier in the Effective Thermal Diffusivity / Conductivity of SiC Fiber Reinforced RBSN," J. Am. Ceram. Soc., **73**, [2], 312, 1990.

[20] R.T. Bhatt and R.E. Phillips, "Thermal Effects on the Mechanical Properties of SiC Fiber-Reinforced Reaction-Bonded Silicon Nitride Matrix Composites," J. Mat. Sci., **25**, 3401, 1990.

[21] R.T. Bhatt, "Oxidation Effects on the Mechanical Properties of a SiC Fiber Reinforced Reaction-Bonded Si_3N_4 Matrix Composites," J. Am. Ceram. Soc., **75**, 406, 1992.

[22] G.E. Hilmas, J.W. Holmes, R.T. Bhatt, and J.A. DiCarlo, "Tensile Creep Behavior and Damage Accumulation in a SiC-Fiber/RBSN-Matrix Composite," in Ceramic Transactions Vol.38 –Advances in Ceramic Matrix Composites, N. Bansal (ed.), ACS, Westerville, OH, pp.291-304, 1993.

[23] A.P.M. Adriaansen, and H. Gooijer, "Comparative Study of the Oxidation of RBSN and RBSN Coated With CVD Si_3N_4," Euro. Ceram., V3, 1989, pp. 569-574.

[24] O. J. Gregory and M. H. Richman, "Thermal Oxidation of Sputter-Coated Reaction-Bonded Silicon Nitride," J. Amer. Ceram. Soc. 67, [5], pp.335-340 (1984).

[25] J. Desmaison, N. Roels, and P. Belair, "High-Temperature Oxidation-Protection CVD Coatings for Structural Ceramics: Oxidation Behavior of CVD-Coated Reaction-Bonded Silicon Nitride," Mater. Sci. and Eng., A121 441-447 (1989).

[26] D.S. Fox, "Oxidation Kinetics of Coated SiC/RBSN," 6th Annual HITEMP Review – 1993 NASA CP 19117 pp. 69-1 to 69-3.

[27] D.S. Fox, "Oxidation Protection of Porous Reaction-Bonded Silicon Nitride," J. Mat. Sci. **29** (21), 5693-5698, 1994.

[28] W. Fohey, R.T. Bhatt, and G.Y. Baaklini, "Burner Rig and Engine Test Results on SiC/RBSN Composites," 6th Annual HITEMP Review – 1993 NASA CP 19117 pp. 68-1 to 68-3.

[29] R.W. Rice, P.F. Becher, S.W. Freiman, and W.J. McDonough, "Thermal Structural Ceramic Composites," Ceram. Eng. Sci. Proc., 1[7-8], pp. 424-443 (1980).

[30] D.K. Shetty, M.R. Pascucci, B.C. Mutsudy, and R.R. Wills, "SiC Monofilament-Reinforced Si_3N_4 Matrix Composites," Ceram. Eng. Sci. Proc. 16[7-8], pp. 632-645 (1985).

[31] W. Foulds, J.F. Lecostaouec, C. Landry, and S. Dipietro, "Tough Silicon Nitride Matrix Composites Using Textron Silicon Carbide Monofilaments," Ceram. Eng. Sci. Proc. 10, [9-10], pp. 1083-1089 (1989).

[32] A.G. Razzel and M.H. Lewis, "Silicon Carbide/SRBSN Composites," Ceram. Eng. Sci. Proc. 12, [7-8], pp. 1304-1317 (1991).

[33] K. Nakano, S. Kume, K. Sasaki, and H. Saka, "Microstructure and Mechanical Properties of Hi-Nicalon Fiber Reinforced Si_3N_4 Matrix Composites," Ceram. Eng. Sci. Proc. 17, [4], pp. 324-332 (1996).

[34] J.W. Holmes,Y. Parks, and J.W. Jones, "Tensile Creep and Creep Recovery Behavior of a SiC Fiber Si_3N_4 Matrix Composite," J. Am. Ceram. Soc., 76 [5] 1281-1293 (1993).

[35] J.W. Holmes, "Tensile Creep Behavior of a Fiber Reinforced SiC-Si_3N_4 Composite," J. Mat. Sci., **26**, 1808-1814 (1991).

List of Tables

List of Figures

Fig. 11 Variation of steady state creep rate with applied stress for 1-D SiC/RBSN composites containing ~24 vol% fibers at 1300^{0}C in nitrogen and oxygen [22].

Fig. 12 Room temperature tensile-stress-strain curves for 1-D and 2-D Hi-Nicalon SiC/RBSN composites containing ~ 24 vol% fibers, and unreinforced RBSN matrix [11].

Fig. 13 Cross sections of a CVD SiC/glass former coated SiC/RBSN monofilament composite after 10 h burner rig testing in air at 1600^{0}C showing stability of carbon core and coating.

Fig. 14 Room temperature tensile stress- strain behavior for 1-D and 2-D HP SiC/ Si_3N_4 composites containing ~30 vol% SiC monofilaments [31].

Fig. 15 Variation of steady-state tensile creep rate with tensile creep stress for monolithic HP-Si_3N_4 at 1315^{0}C and HP-SiC/Si_3N_4 composites tested at 1350^{0}C in air [34, 35].

Table I Room temperature physical and mechanical properties for SiC/RBSN composites [8-10, 14].

Property	**1-D**	**2-D**
Physical Properties		
Fiber content, %	24-30	24-30
Density, gm/cc	2.2-2.4	2.2-2.4
Porosity, %	30-40	30-40
Flexural Properties@		
Elastic Modulus, GPa	182±10	NA
Matrix Cracking Stress, MPa	206±40	NA
Matrix Cracking Strain, %	0.1	NA
Ultimate Strength, MPa	965±138	NA
Ultimate Strain, %	1.2	NA
Tensile Properties		
Elastic Modulus, GPa	186±20	118±15
Matrix Cracking Stress, MPa	227±41	130±30
Matrix Cracking Strain, %	0.13	0.1
Ultimate Tensile Strength, MPa	690±138	316±62
Ultimate Tensile Strain, %	1	0.6
Poisson's Ratio	0.21	NA
Compression Properties		
Elastic Modulus, GPa	180±7	157±5
Ultimate Tensile Strength, MPa	1752±207	722±74
Ultimate Tensile Strain, %	1	0.5
Shear Properties		
Shear Modulus, GPa	31±3	NA
Interfacial Shear Strength*, MPa	11±7	NA
Interlaminar Shear Strength#, MPa	40±4	NA
Fracture Toughness, MPa$(m)^{1/2}$	13	NA

@ 4-point flexural test, specimen size: 3mm (T) x 4mm (W) x 50 mm (L)

NA-Data not available

Double notch shear test

* Fiber push-out method

Table-II Room temperature tensile properties of unidirectional SiC/RBSN composites (V_f~0.24) [17]

Room-temperature properties	As-fabricated[a] (not cycled)	After 5 cycles in nitrogen[b] 25 to 1400°C	After 5 cycles in oxygen[b] 25 to 1400°C
Elastic modulus, GPa	178±16	186	173
Tensile strength, MPa			
First matrix	220±24	213	138
Ultimate	680±62	551	138
Strain to failure, %			
First matrix	0.12	0.11	0.08
Ultimate	0.45	0.40	0.08

a - Average of 5 specimens
b - Average of 3 specimens

Table-III Thermal property data for 1-D SiC/RBSN composites in nitrogen [18, 19].

Property	**Temperature, ^{0}C**			
	25	**600**	**1000**	**1400**
Thermal Properties				
Thermal Expansion				
In-Plane, $10^{-6}/^0$C	NA	3.1	3.6	3.8
Through-the -Thickness, $10^{-6}/^0$C	NA	2.9	3.2	3.7
Specific Heat J/kg-K	675	1250	1312	1330
Thermal Diffusivity				
In-Plane, 10^6 m^2/sec	7	3.3	2.8	2.5
Through-the -Thickness, 10^6 m^2/sec	2.5	1.8	1.8	1.8
Thermal Conductivity				
In-Plane, W/m-K	10	9.0	8.0	7.0
Through-the -Thickness, W/m-K	4.5	4.5	4.5	4.5

Table-IV Thermal property data for 2-D SiC/RBSN composites in nitrogen.

Property	Temperature, ^{0}C			
	25	600	1000	1400
Thermal Properties				
Thermal Expansion				
In-Plane, $10^{-6}/^0$C	NA	3.3	3.9	3.9
Specific Heat, J/kg-K	680	1160	1240	1270
Thermal Conductivity				
Through-the -Thickness, W/m-K	4.59	4.0	4.0	3.8

Table V. Physical property data for Hi-Nicalon SiC/RBSN composites [11].

Interface coating	Fiber lay-up	Fiber volume, %	Density, gm/cc	Porosity, %
BN/SiC	0	24±1	1.96±0.03	36
BN/SiC	0/90	24±2	1.94±0.01	37

Table VI. Room temperature tensile property data for SiC/RBSN composites. [11]

Interface coating	Fiber lay-up	Fiber volume, %	Proportional limit stress, MPa	Proportional limit strain, %	Elastic modulus, GPa	Ultimate tensile strength, MPa	Ultimate tensile strain, %
BN/SiC	0	24±1	290±21	0.28±0.02	105±1	329±8	0.27±0.13
BN/SiC	0/90	24±2	88±18	0.12±0.03	73±3	133±22	0.35±0.09

Table VII Physical and mechanical properties for HP SiC/Si_3N_4 composites[10, 31,34]

Property	Temperature, ^{0}C	
	25	1350-1370
Physical Properties		
Fiber content, %	30	30
Density, gm/cc	3.2	NA
Flexural Properties@		
Elastic Modulus, GPa	319	140
Matrix Cracking Stress, MPa	528	
Matrix Cracking Strain, %	0.16	
Ultimate Strength, MPa	620	366
Ultimate Strain,%	0.28	0.5
Tensile Properties		
Elastic Modulus, GPa	316	260
Matrix Cracking Stress, MPa	348	84
Matrix Cracking Strain, %	0.11	0.03
Ultimate Tensile Strength, MPa	476	290
Ultimate Tensile Strain, %	0.6	0.22
Shear Properties		
Interfacial Shear Strength*, MPa	29±7	NA
Interlaminar Shear Strength#, MPa	59	NA

@ 4-point flexure test, specimen size: 3mm (T) x 4mm (W) x 50 mm (L)

3-point short beam flexural test

* Fiber push-out method

NA-data not available

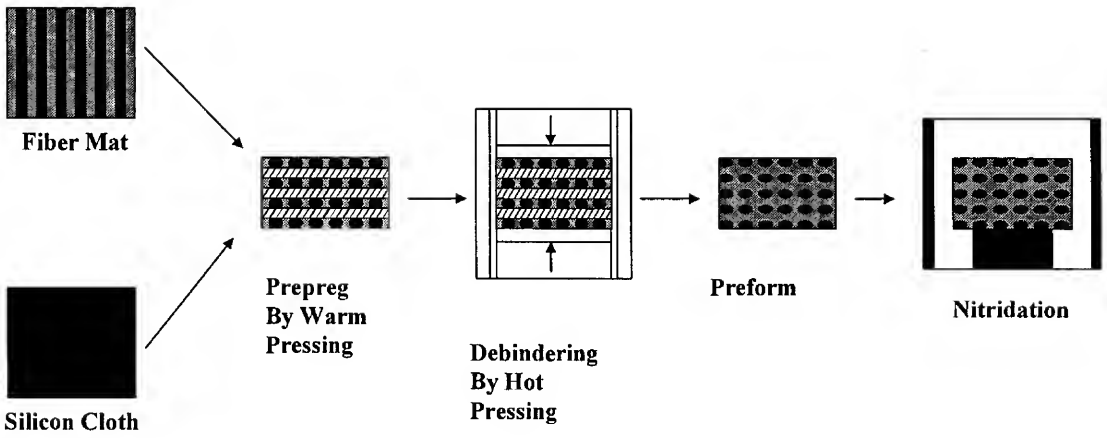

Fig. 1 Fabrication steps for SiC fiber reinforced reaction-bonded silicon nitride composites.

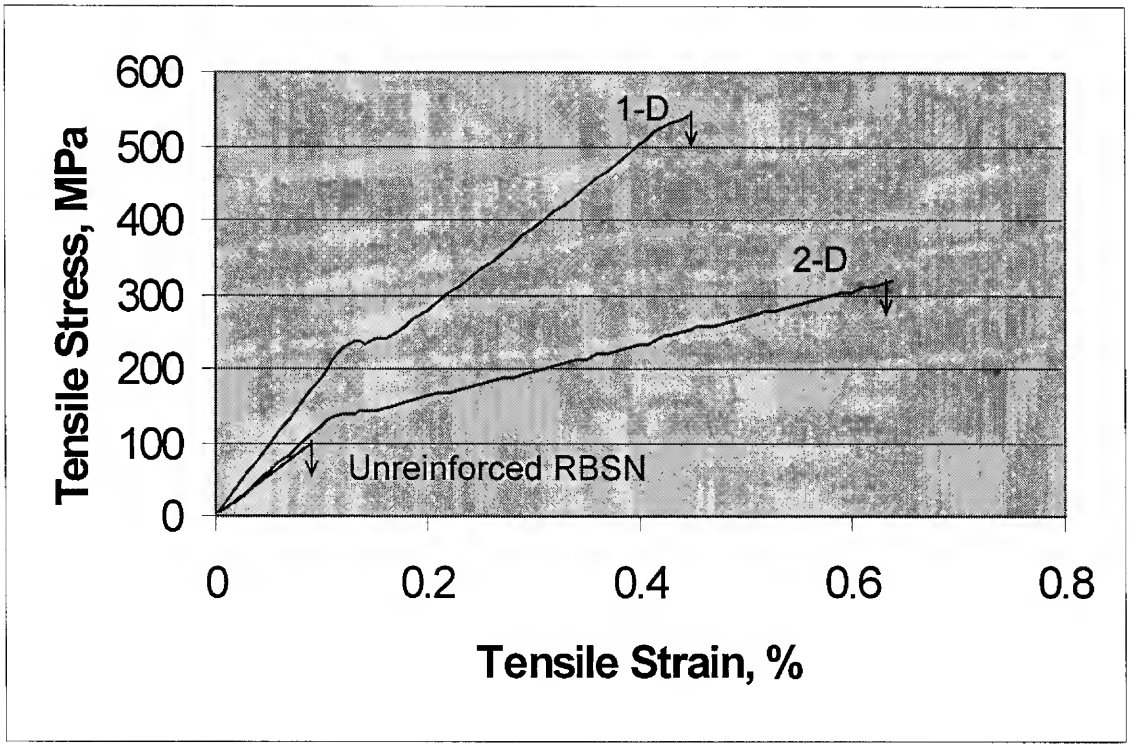

Fig. 2 Room temperature tensile stress-strain curves for 1-D and 2-D SiC/RBSN composites containing ~24 vol% fibers, and unreinforced RBSN [8, 9].

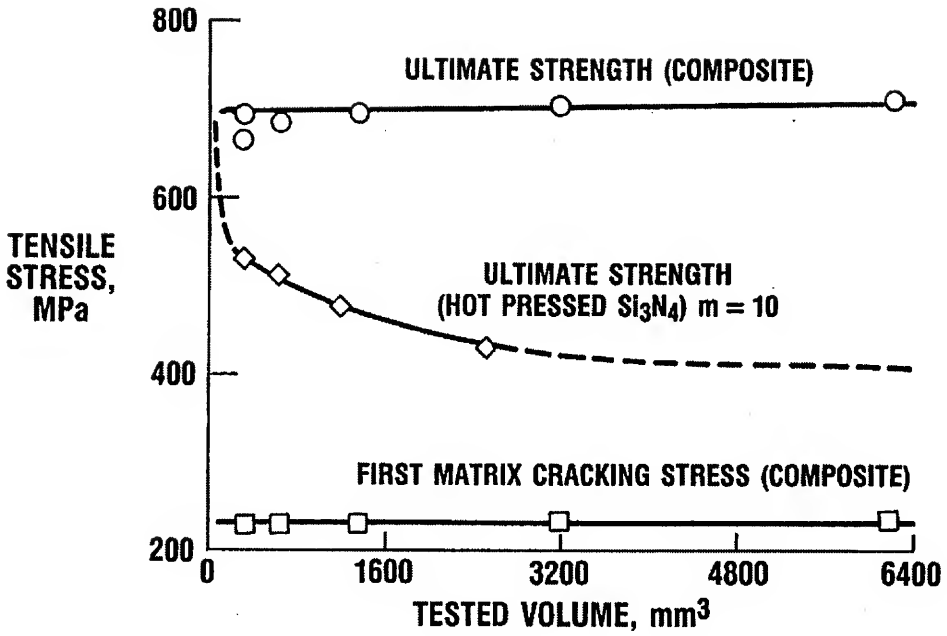

Fig. 3 Variation of room temperature tensile strength with tested volume for 1-D SiC/RBSN composites containing ~24 vol% fibers and hot- pressed silicon nitride [8, 15].

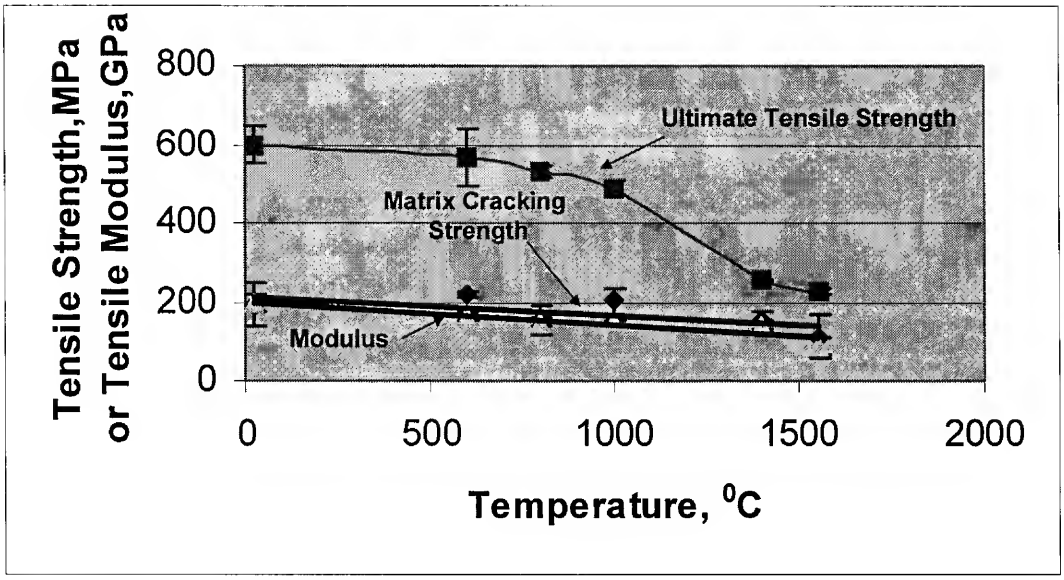

Fig. 4 Variation of mechanical properties with temperature for 1-D SiC/RBSN composites containing ~24 vol% fibers tested in air [16].

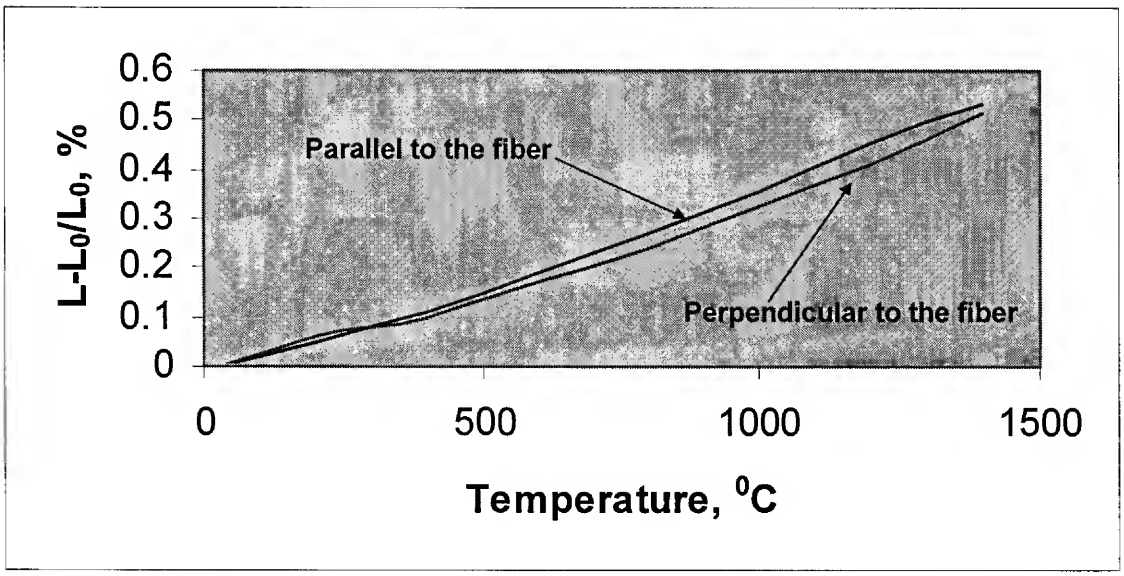

Fig. 5 Linear thermal expansion curve during heating in nitrogen for 1-D SiC/RBSN composites containing ~24 vol% fibers measured parallel and perpendicular to the fibers [17].

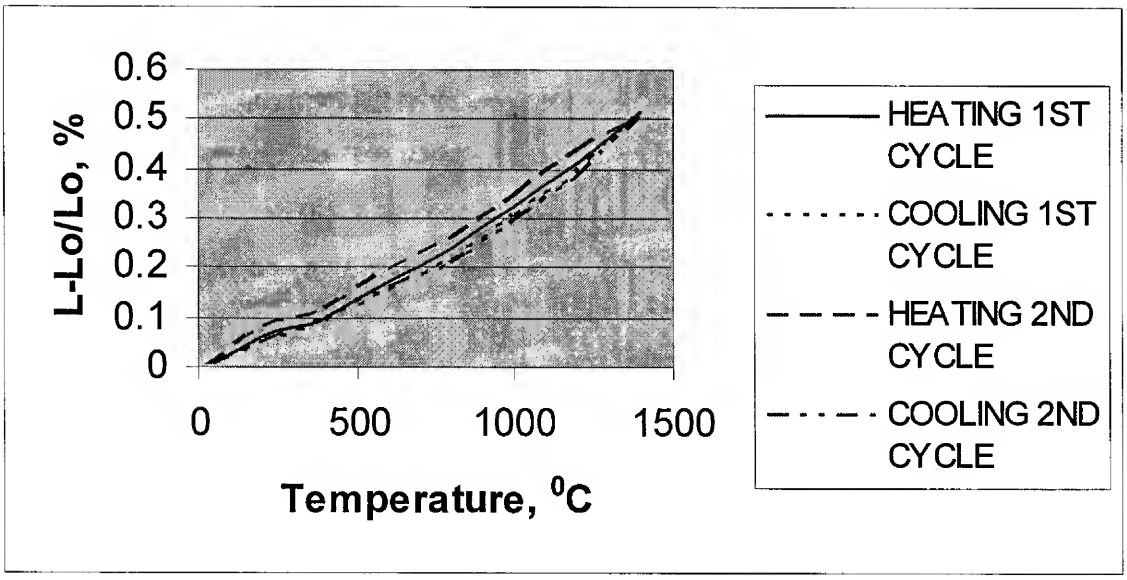

(a)

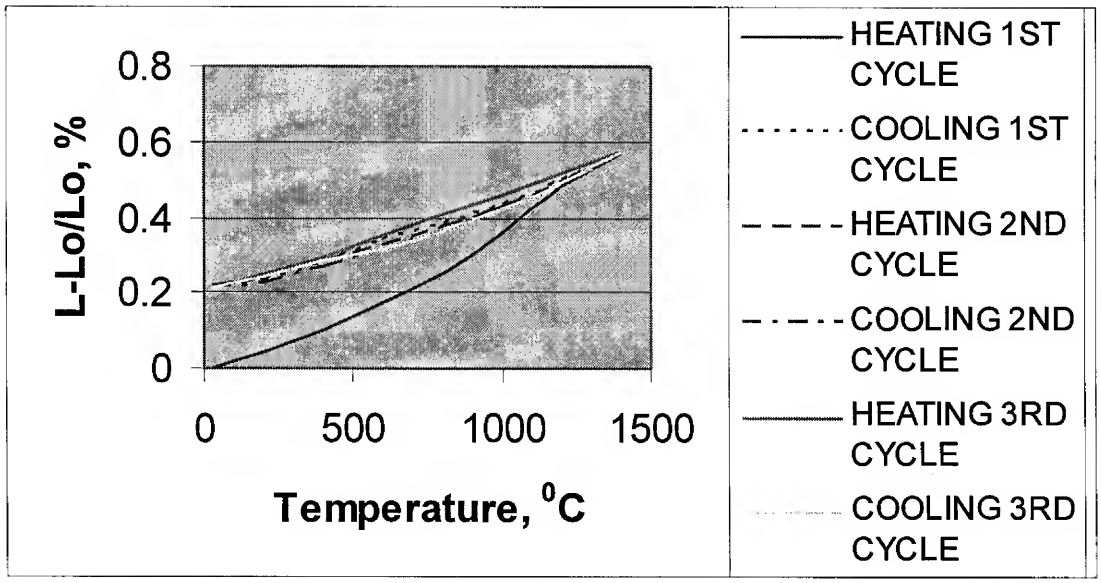

(b)

Fig. 6 Thermal expansion and contraction curves for a 1-D SiC/RBSN composite containing ~24 vol% fibers measured transverse to the fibers in (a) nitrogen, and (b) oxygen showing influence of internal oxidation [17].

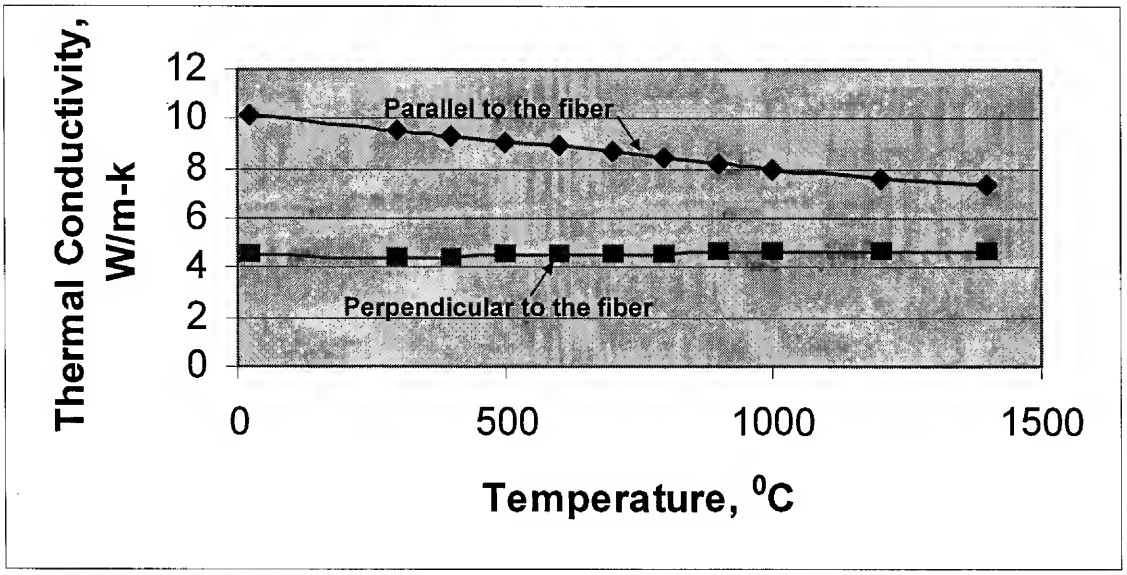

Fig. 7 Variation of thermal conductivity with temperature for 1-D SiC/RBSN composites containing ~24 vol% fibers measured in nitrogen [18, 19]

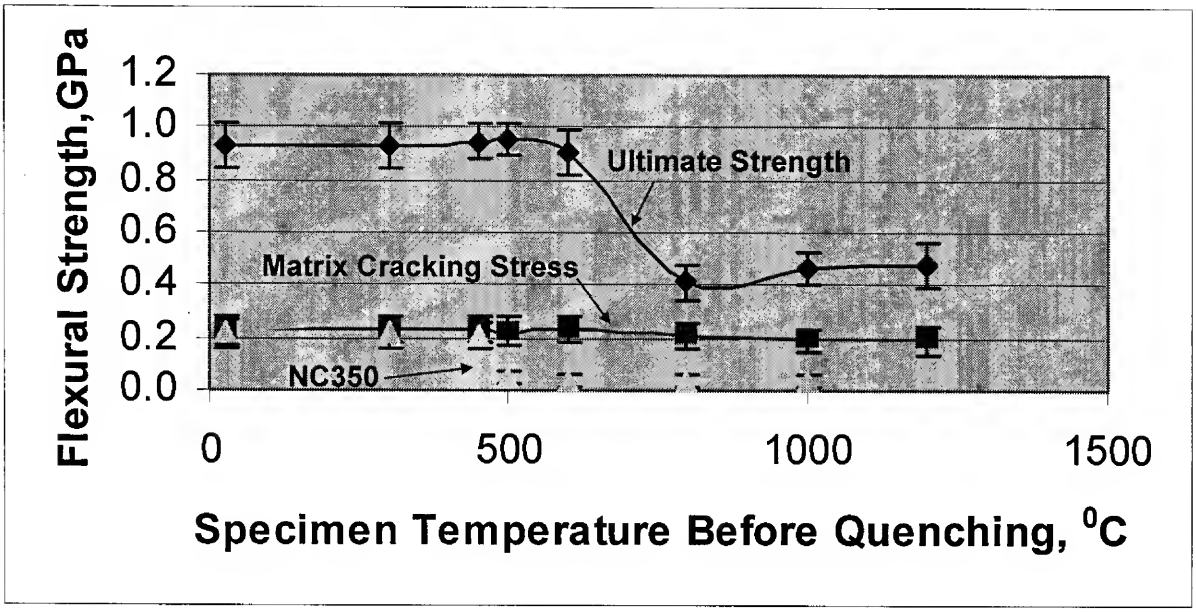

Fig. 8 Room temperature 4-point flexural strengths for 1-D SiC/RBSN composites containing ~30 vol% fibers and monolithic RBSN (NC350) after quenching [20].

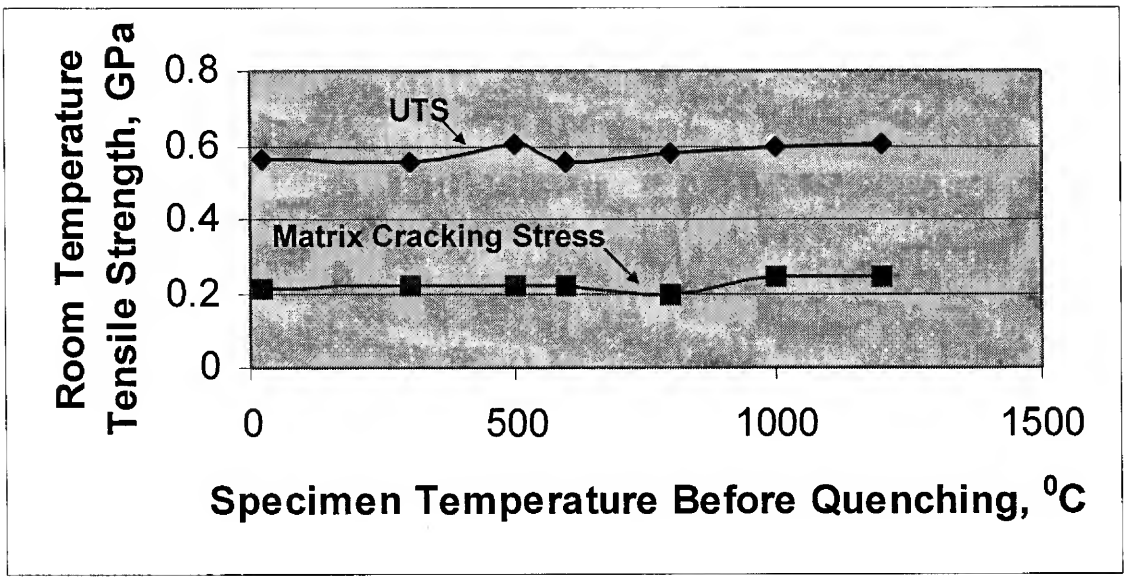

Fig. 9 Room temperature tensile strengths for 1-D SiC/RBSN composites containing ~30 vol% fibers after quenching [20].

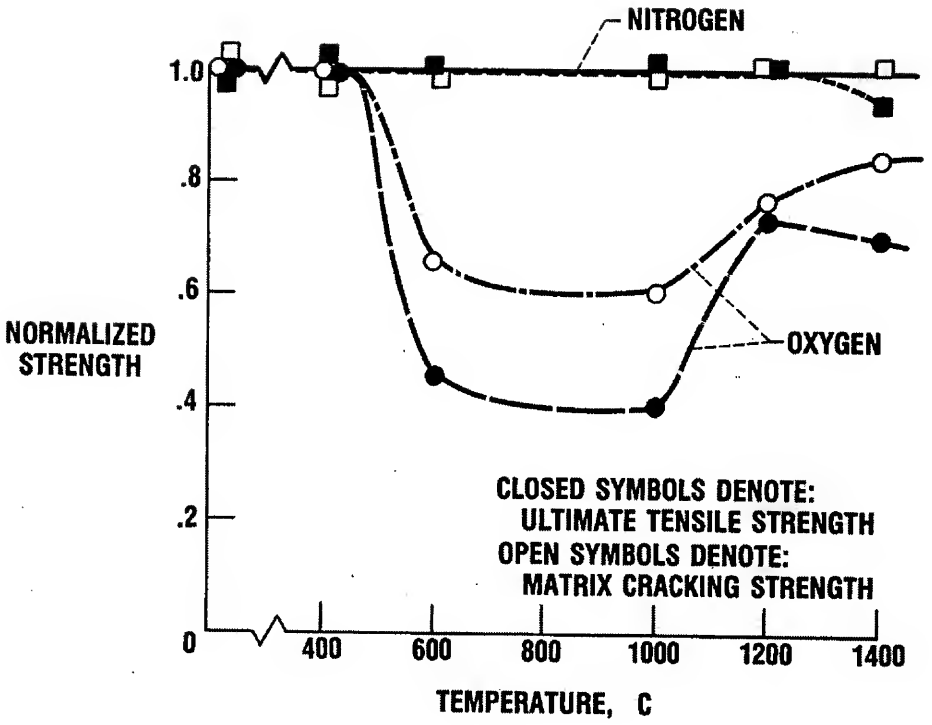

Fig. 10 Influence of 100hr exposure in nitrogen and oxygen environments on room temperature tensile properties of 1-D SiC/RBSN composites containing ~24 vol% fibers [21]. Normalized strength is defined as the ratio of room temperature tensile strength of the environmentally exposed specimens to that of the as-fabricated specimens.

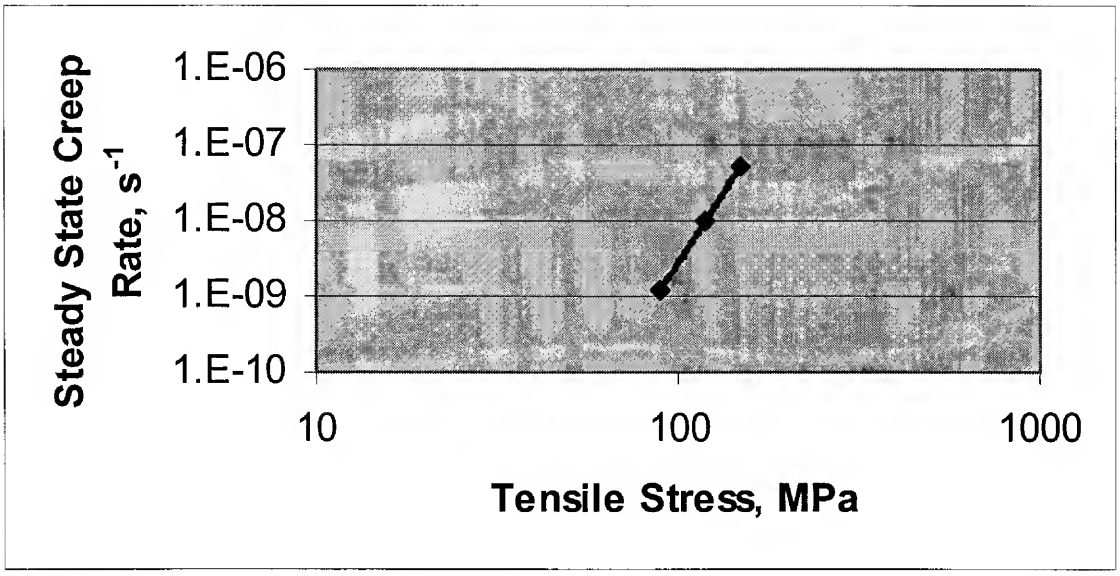

Fig. 11 Variation of steady state creep rate with applied stress for 1-D SiC/RBSN composites containing ~24 vol% fibers at 1300^0C in nitrogen and oxygen.[22]

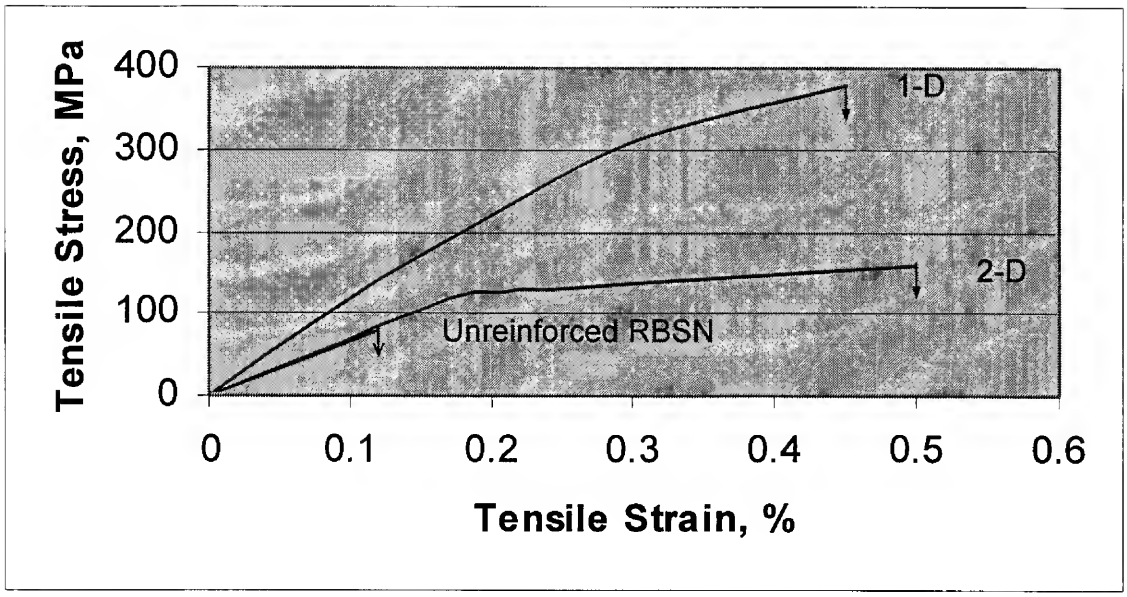

Fig. 12 Room temperature tensile-stress-strain curves for 1-D and 2-D Hi-Nicalon SiC/RBSN composites containing ~ 24 vol% fibers, and unreinforced RBSN matrix [11].

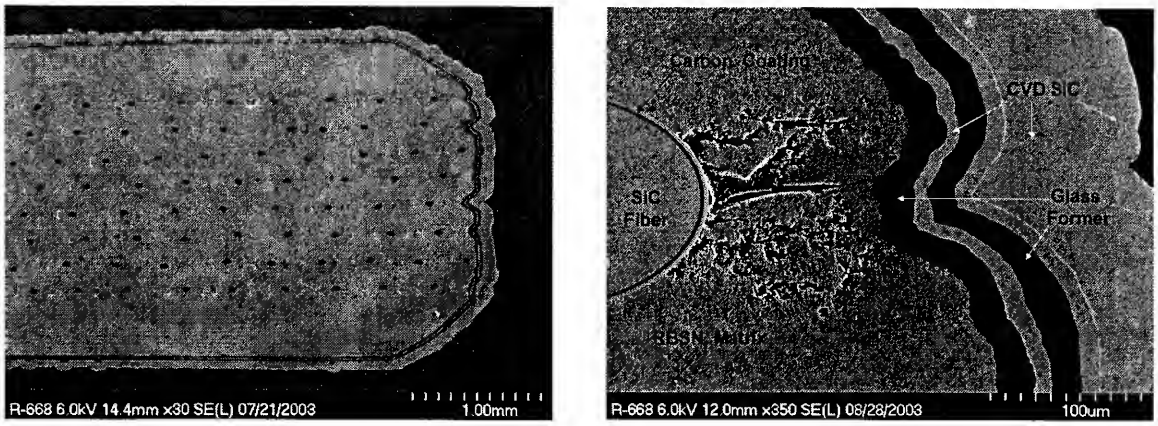

Fig. 13 Cross sections of a CVD SiC/glass former coated SiC/RBSN monofilament composite after 10 h burner rig testing in air at 1600^0C showing stability of carbon core and coating.

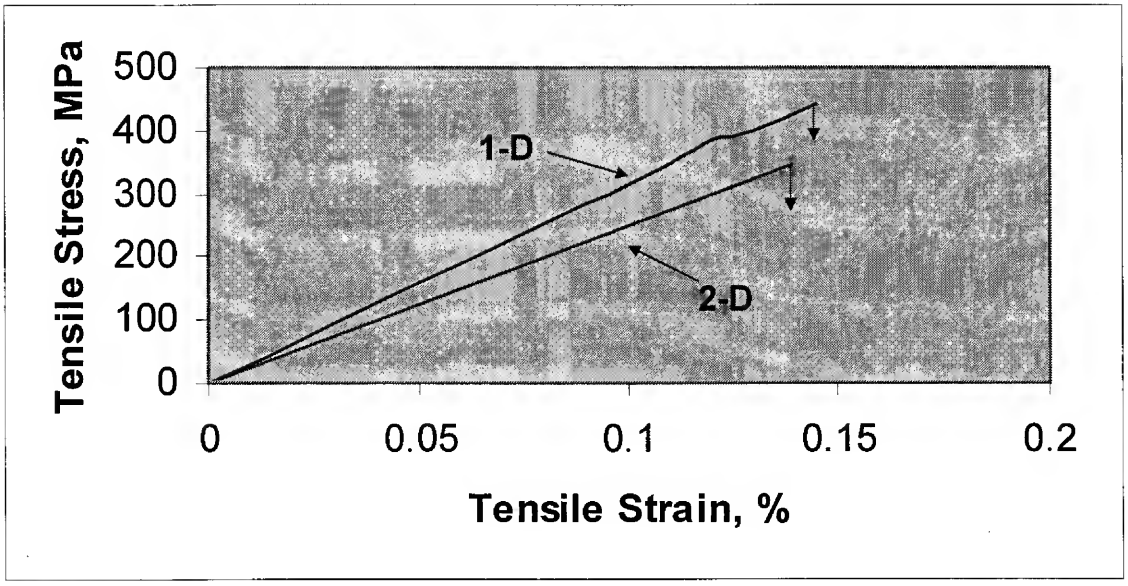

Fig. 14 Room temperature tensile stress strain behavior for 1-D and 2-D HP SiC/ Si_3N_4 composites containing ~30 vol% SiC monofilaments [31]

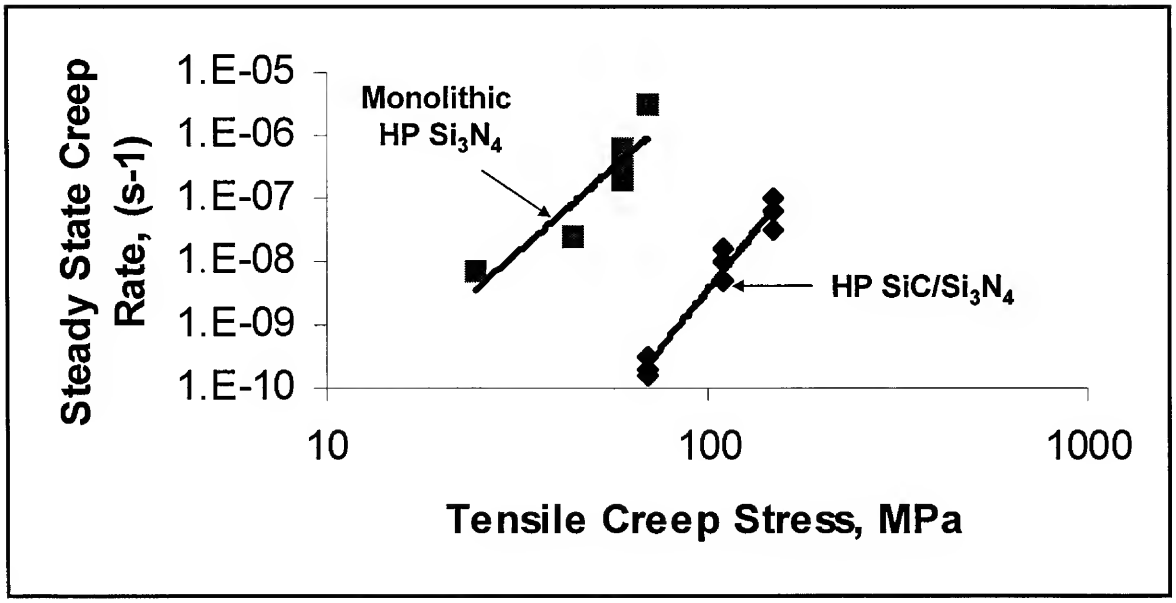

Fig. 15 Variation of steady-state tensile creep rate with tensile creep stress for monolithic HP-Si_3N_4 at 1315^{0}C and HP-SiC/Si_3N_4 composites tested at 1350^{0}C in air [34, 35].